

Breaking the biofilm barrier: CRISPRi-guided investigation of *Pseudomonas aeruginosa* susceptibility to natural products

By
Sherrie Ying Wu

A senior honors thesis submitted in partial fulfillment of the requirements for the degree of

Bachelor of Science
(Biochemistry, Honors in the Major)

at the
UNIVERSITY OF WISCONSIN-MADISON

2025

Acknowledgements

I started college not really knowing what research meant, and here I am four years later, having finished a senior (honors!!) thesis. I would like to extend my thanks to the Undergraduate Research Scholars program, which gave me a chance to enter the world of research solely based on my curiosity about it. Thank you, Dr. Tim Bugni, for believing in me and welcoming me into your lab as a junior and gifting me with a project that truly challenged me and helped me grow as a researcher. I thank Chris for helping guide me through this project– even though you claim I know more about biochemistry than you, I still appreciated being confused together when experiments didn't work. Thank you, Doug, for helping me with my experiments and letting me bug you all the time. Thank you, Bugni lab members, for being a great support system and for always making me laugh when I come into lab.

I would also like to thank my first mentor, Dr. Thy Nguyen, who welcomed me to Dr. Lindsay Kalan's lab with open arms and taught me how to open lids with one hand (while having perfect sterile technique), among many other important lab and life skills. Your support helped me believe in myself and truly see myself belonging in science. I would like to thank Dr. Kalan for also welcoming me into your lab as a freshman with no experience and investing in me from the ground up. Thank you for being one of my biggest advocates throughout my college career, and as I applied to medical school. I also thank Kalan lab members, past and present.

I thank my advisors at the Mercile J. Lee Scholarship Program who have cheered me on and supported my research endeavors throughout my undergraduate career. Thank you Ryan, Emma, Lena, Kao Yong, and other MJLSP staff.

I thank my parents, who immigrated to the United States so that I could have opportunities like this one. I thank you and my older brother for always supporting me throughout my life. I thank my friends who supported me and my research- attending symposiums, asking questions, and believing in me. Thank you, Kung, for your wholehearted support in my research, school, pre-med, etc., endeavors. You always understand when I forget about something I needed to do in the lab and stuck with me for too many late evenings. Thank you for also teaching me how to code for this project. Linux is still hard.

Table of Contents

Acknowledgements	1
Table of Contents	2
Thesis Abstract	3
Introduction	4
Materials and Methods	7
Results	10
Discussion	18
Works Cited	22
SI	Upon Request

Thesis Abstract

Antibiotic resistance is a growing concern, with pathogens such as *Pseudomonas aeruginosa* evolving resistance to clinical treatments. Furthermore, our race against antibiotic resistance is worsened by a slowdown in novel antibiotic discovery. The Gram-negative bacterium *P. aeruginosa* often causes infections in patients with cystic fibrosis and poses a particular threat due to its ability to form biofilms, which are stable supercellular structures that adhere to surfaces and enhance resistance to antibiotics. However, natural products are promising sources for discovering new antimicrobial compounds. This project investigates the mechanism by which a recently discovered antibacterial natural product and a semi-synthetic derivative inhibit *P. aeruginosa* and its biofilm formation. Full genome CRISPR-interference (CRISPRi) knockdown strains of *P. aeruginosa* PA14 were utilized to identify the genetic and biochemical targets of the natural product and its analog. By elucidating the mechanism of how biofilm formation is inhibited, this research aims to reveal vulnerable genes and pathways that can be targeted for future antibiotic development, with implications for treating *P. aeruginosa* and potentially other comparable pathogens.

Breaking the biofilm barrier: CRISPRi-guided investigation of *Pseudomonas aeruginosa* susceptibility to natural products

Introduction

Antibiotic resistance has become a growing concern, and as a result, infections are more difficult to treat. Contributors to this growing crisis include overuse of antibiotics in agriculture and misuse of antibiotics in humans, as well as a lack of new drug development¹. In 2019, there were estimated to be 14 million infection-related deaths², with 4.5 million of them attributed to antibiotic resistance³.

One of the microorganisms contributing to antibiotic-resistant infections is *Pseudomonas aeruginosa*, a ubiquitous Gram-negative bacterium and opportunistic pathogen that poses a threat to human health. *P. aeruginosa* has been recognized as a priority pathogen for developing new antibiotics by the World Health Organization⁴ and is one of the most prevalent pathogens in medical settings, causing more than 50% of healthcare-acquired infections⁵. It can cause pneumonia, catheter-related infections, implant-related infections, and skin burn infections⁵. These infections may be fatal in immunocompromised patients, such as those with cancer, human immunodeficiency virus (HIV), or recent surgical procedures⁶.

P. aeruginosa is a versatile pathogen, developing two distinct lifestyles, planktonic and sessile⁵. In the planktonic state, bacterial cells are free and mobile, exploring their environment for nutrients. In the sessile state, *P. aeruginosa* forms a biofilm, where the bacterial colonies adhere to surfaces and form clusters that secrete an adhesive and protective matrix. In this communal state, cells share nutrients and are protected from harmful conditions^{5,7}, which enhances *P. aeruginosa*'s pathogenicity and antibiotic resistance in clinical settings.

To address the issue of the difficulty in treating *P. aeruginosa* infections and biofilms, this project aims to follow up on a novel antibacterial natural product discovered in the Bugni laboratory, found to inhibit *P. aeruginosa* biofilm formation. Natural products are compounds made by living organisms and are the most promising sources of novel antimicrobial compounds⁸. The novel antibacterial natural product of interest was produced by a bacterium in the family Micromonosporaceae, which was isolated from a sponge on the coast of Florida. After structure elucidation of the natural product and creation of semi-synthetic analogs, experiments revealed that three semi-synthetic analogs potentially inhibited the biofilm formation of *P. aeruginosa*. The promising results from a *P. aeruginosa* biofilm assay conducted with one of the semi-synthetic analogs are shown in **Figure 1**, where 0.3125 μM of the compound was enough to elicit a similar anti-biofilm activity as the positive control antibiotic. The natural products and semi-synthetic analogs will be referred to as PANPs, for *P. aeruginosa*-targeting natural products.

In this study, we provide insight into the potential mechanism of action of two PANPs: PANP2, an original natural product, and S-PANP2, a semi-synthetic derivative of PANP2 that has been modified with an amino acid-like moiety. Uncovering the proposed mechanisms was achieved by performing a CRISPR-interference (CRISPRi) library growth experiment using a Mobile-CRISPRi full genome knockdown library of *P. aeruginosa* strain PA14 (here often referred to simply as PA14), which is a laboratory reference strain containing a hyper-virulent phenotype⁹. CRISPRi is a genetic tool that involves the controlled inhibition of gene

expression¹⁰. By using programmable single guide RNAs (sgRNAs) that can be thought of as 'barcodes' for genes, we can evaluate the differential survival- and thus fitness- of various gene knockdowns/barcodes when exposed to PANP2 and S-PANP2. This may provide insights into which genes and pathways are more sensitive to PANPs, as well as which gene knockdowns may confer greater fitness against PANPs. This experiment was performed with the assistance of the Dr. Jason Peters Lab at the UW-Madison School of Pharmacy, following a protocol first published by Ward et al.¹¹

In all, by uncovering the specific mechanism of action of PANPs and the genes and pathways they target, we will deepen our understanding of *P. aeruginosa* pathogenicity, specifically biofilm formation. This understanding can then be applied to further antibiotic development against *P. aeruginosa* and pathogens with similar characteristics.

Note: The structures of the novel natural product (PANP2) and its semi-synthetic analog (S-PANP2) were not explicitly included in this thesis to protect intellectual property. Please reach out to Sherrie Wu ([sywu@wisc.edu](mailto:syw@wisc.edu)) or Dr. Tim Bugni (tim.bugni@wisc.edu) for more information.

Biofilm Activity of PANP Analog

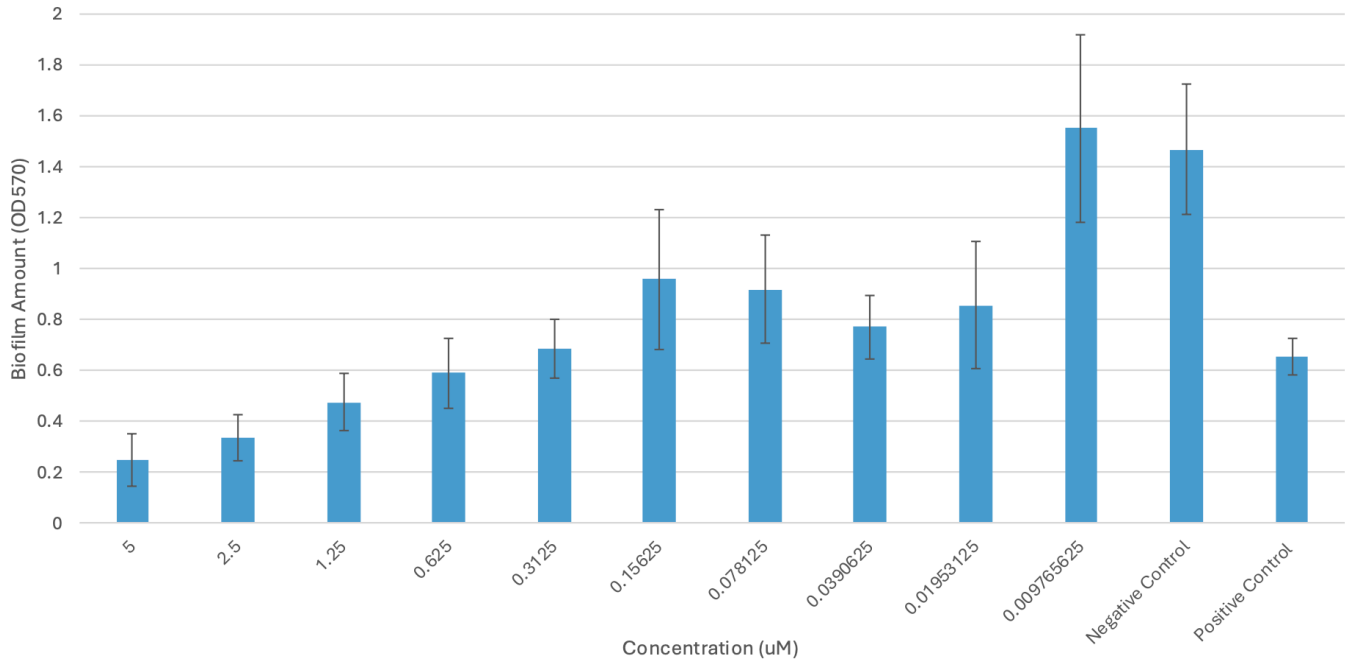


Figure 1. Bar Graph Showing Effects of a PANP on *P. aeruginosa* Biofilm Formation. This data was obtained using a biofilm assay, measuring how different dilutions of a PANP analog of interest, negative control, and positive control (x-axis) affect biofilm formation (OD₅₇₀, y-axis). Notably, when this PANP's concentration is tested at 0.3125 μ M and above, it is as or more effective than the positive control, a clinically-prescribed antibiotic. Figure courtesy of Chris Roberts (unpublished).

Materials and Methods

PA14 Growth Media and Carbon Preference

Based on recommendations from the Peters lab, it was determined that the defined growth medium to be used for the library growth experiment would be the 3-(N-morpholino)propanesulfonic acid (MOPS) EZ Rich Defined Media (EZRDM) from Teknova¹², with succinate as the carbon source.

To identify the optimal succinate concentration for wild-type (WT) PA14 growth in MOPS EZRDM, an overnight growth curve was set up in a 96-well plate, where PA14 was grown in differing concentrations of succinate. First, PA14 was streaked onto lysogeny broth (LB) agar¹³ and incubated overnight at 37 °C. Using a 96-well plate setup, seven different concentrations of succinate were tested in triplicate (in mM): 10, 20, 30, 40, 50, 60, and 75. Wells were inoculated with PA14 with a starting optical density at 600 nm (OD₆₀₀) of 0.1. The 96-well plate was incubated overnight in a Tecan Infinite 200 Pro plate reader at 37 °C, shaking at 200 rotations per minute (rpm) for 18 hours. OD₆₀₀ measurements were taken every 850 seconds, and data points were used to create growth curves by succinate concentration in Excel. Plain MOPS EZRDM was used as the blank. The chosen succinate concentration was then used for all subsequent experiments with MOPS EZRDM.

Doubling time for WT PA14 in the selected concentration of succinate was found by finding the best-fit linear regression of time versus ln(OD₆₀₀). Two timepoints and their corresponding OD₆₀₀ measurements within the line were chosen, and **Equations 1 and 2** were used to determine doubling time.

$$r = \frac{\ln\left(\frac{OD_{600,t2}}{OD_{600,t1}}\right)}{t2-t1}, \text{ where } t2 > t1 \quad (1)$$

$$\text{doubling time} = \ln\left(\frac{2}{r}\right) \quad (2)$$

Determination of 25% Inhibition Concentrations

In order to execute the library growth experiment according to Ward et al.¹¹, we needed to determine the concentration at which PANP2, S-PANP2, and the positive control antibiotic achieved about 25% growth inhibition of WT PA14. Ciprofloxacin (Acros Organic; now Thermo Fisher) was chosen as the positive control antibiotic¹⁴. Inhibition assays were performed in 96-well plates to generate dose-response curves. To prepare for the inhibition assays, PA14 was streaked onto LB agar and incubated overnight at 37 °C. A single colony was then picked and used to inoculate MOPS EZRDM + 40 mM succinate. The liquid culture was incubated overnight at 37 °C with shaking at 200 rpm.

For the inhibition assays, the antibiotic and each PANP were tested in duplicate. Across multiple experiments, the range of concentrations tested includes: 0.000305-40 µg/mL for ciprofloxacin; 0.03-3000 µM for PANP2; and 0.3-3000 µM for S-PANP2. The ciprofloxacin and PANPs were dissolved in dimethyl sulfoxide (DMSO) before being added to the MOPS EZRDM + 40 mM succinate media. The concentration of DMSO was kept below 5% and ideally was below 1% (v/v). The negative control samples were made by adding the highest corresponding amounts of DMSO that were added to the experimental or positive control conditions, into the

growth medium. Liquid culture of PA14 was then added to each well so that the starting OD₆₀₀ of each well was equal and about 0.1.

The 96-well plates were incubated overnight at 37 °C, shaking at 200 rpm. OD₆₀₀ values were measured after growth to quantify relative inhibition, and values were fit to a dose response curve using Kemmer and Keller's sigmoid fitting curve from "Nonlinear least-squares data fitting in Excel spreadsheets"¹⁵. The 25% inhibition concentrations for ciprofloxacin, PANP2, and S-PANP2 were found by estimating the concentration that corresponded to 0.75 times the maximum "y_{calc}" value, which corresponded to the least inhibitory concentration on the dose response curve.

Library Growth Experiment

The *Pseudomonas aeruginosa* PA14 full genome CRISPRi library was obtained from the Jason Peters Lab in the University of Wisconsin School of Pharmacy¹⁶. Methods for the library growth experiments generally follow what was outlined by Ward et al¹¹. The initial PA14 CRISPRi library revival was done by adding 50 μ L of frozen stock (OD₆₀₀ = 15) in 50 mL of MOPS EZRDM + 40 mM succinate (OD₆₀₀ = 0.015) and incubation at 37C, 200 rpm in a 250 mL flask until OD₆₀₀ was approximately 0.2 (~4.5 hr, T0). This initial culture was diluted into four different conditions in triplicate. All conditions were diluted to an OD₆₀₀ of 0.02 solution containing 4 mL MOPS EZRDM + 40 mM succinate + 1.03 mM isopropyl β -D-1-thiogalactopyranoside (IPTG).

Experimental conditions included PANP2 and S-PANP2, while the positive control contained ciprofloxacin. The negative control replicates contained the maximum amount of DMSO used to add the PANPs or antibiotic to the media, and total DMSO concentration was kept below 1% (v/v) for all samples. Samples were grown to saturation by incubating for 18 hours at 37 °C with shaking (T1). The cultures were then diluted back to OD₆₀₀ = 0.02 and incubated again for 18 hours in the same conditions (T2). 1 mL of culture was collected from each sample at T1 and T2 (10 mL of T0); cells were pelleted in duplicate by centrifugation at 16,000g for 1 minute and stored at -20 °C.

Sequencing Library Samples

Methods for sequencing library samples also generally follow what was outlined by Ward et al¹¹. DNA was extracted from T0 and T2 pellets using the GeneJet DNA Purification Kit (Thermo) following the manufacturer's protocol, resuspending in a final volume of 100 μ L with an average yield of 86 ng/ μ L. The sgRNA-encoding region with Illumina adapters was amplified using low-cycle PCR (16 cycles) and eluted in a final concentration of ~19 ng/ μ L. The primers oJMP697 and oJMP698¹¹ were used. Amplification was confirmed by running PCR products on a 2% agarose gel with 1kb Plus DNA Ladder (NEB).

Samples were sequenced by the UW-Madison Biotech Center Next Generation Sequencing Core facility. PCR products were amplified with nested primers containing i5 and i7 indexes and Illumina TruSeq adapters, followed by bead cleanup, quantification, pooling, and running on a Novaseq 6000 (150 bp paired-end reads).

Library Data Analysis

Counting sgRNA sequences was performed via data preprocessing¹⁷, and relative fitness scores (\log_2 Fold Change (FC)) were computed using *edgeR*. Volcano plots were created in R using *edgeR* and *ggplot*, comparing all conditions against the negative control conditions. For more information on digital resources and links to custom scripts, see SI (Supplemental Methods).

The top 50 gene knockdown hits that were either more sensitive or had increased fitness in any condition (ex. ciprofloxacin, PANP2, S-PANP2) were identified and analyzed. The *Pseudomonas aeruginosa* UCBPP-PA14 BioCyc database¹⁸ was used to identify genes and proteins from the general gene code (i.e., PA14_RS#####), in conjunction with the National Center for Biotechnology Information (NCBI) Basic Local Alignment Search Tool (BLAST)¹⁹. We identified all gene codes with a net \log_2 FC change above 1 (**Table S1**).

Results

PA14 Grows in a Range of Succinate Conditions

Unlike many bacteria that prefer glucose as a primary carbon source, environmental *P. aeruginosa* prefers succinate, which is also readily available in the airways of patients with cystic fibrosis²⁰. For instance, when grown in the presence of both glucose and succinate, *P. aeruginosa* represses the central glucose catabolism pathway until succinate is consumed²¹.

Thus, to determine optimal succinate concentrations in our defined MOPS EZRDM growth medium, we tested succinate concentrations ranging from 10 mM to 75 mM. We found that, across all concentrations tested, WT PA14 grew well over 18 hours. As seen in **Figure 2**, all succinate concentrations resulted in similar growth patterns: a short lag phase followed by an exponential phase. Then, growth began to plateau around an OD₆₀₀ of 1.15, with only the PA14 growth in the 10 mM condition dropping around 14 hours and ending with an OD₆₀₀ value of 0.916 at the conclusion of the experiment.

We chose to use 40 mM succinate in our growth medium moving forward to follow literature precedent, and, because at this concentration, other carbon catabolism pathways are repressed^{22,23}. The doubling time of WT PA14 in MOPS EZRDM + 40 mM succinate was calculated to be 1.16 hours, or 69.6 minutes.

PA14 Varying [Succinate] Growth Curves

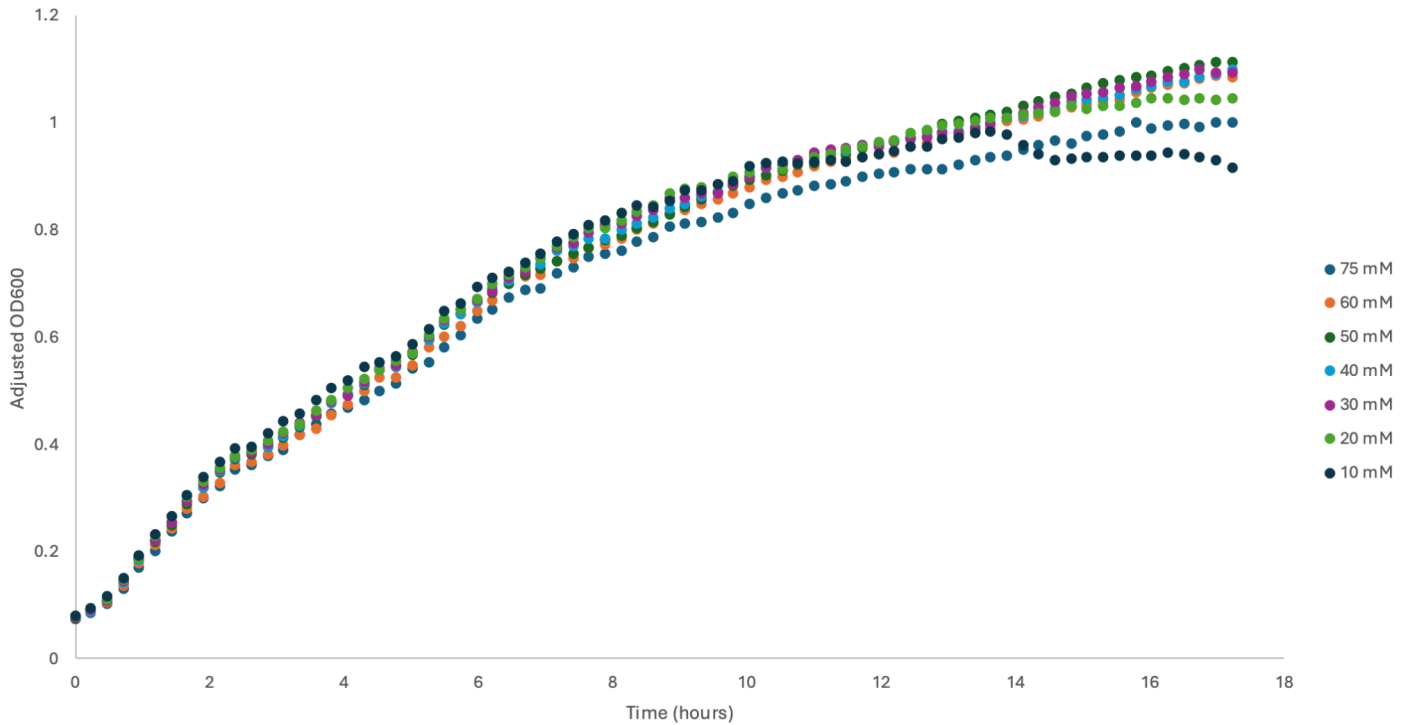


Figure 2. Wild-type *P. aeruginosa* PA14 Growth Curve Across Succinate Concentrations. WT PA14 was grown in MOPS EZRDM (Teknova) at varying succinate concentrations, ranging from 10 mM to 75 mM. Growth was recorded using OD₆₀₀ measurements with a Tecan Infinite 200 Pro plate reader.

PANPs Split on Effective PA14 Inhibition

To identify the appropriate concentrations of our PANPs and positive control antibiotic ciprofloxacin to be used in the library growth experiments, we tested the dose response of WT PA14 against a range of concentrations of these compounds, aiming to find the concentrations at which PA14 was inhibited by about 25%.

As expected for a positive control, we found that ciprofloxacin had a strong dose response against PA14 (**Figure 3a**). The 25% inhibitory concentration of ciprofloxacin for PA14 in MOPS EZRDM + 40 mM succinate medium was about 0.009 µg/mL.

Despite PANP2's potent *P. aeruginosa* biofilm inhibition, PA14 exhibited a weak dose-response to it (**Figure 3b**). Even at the highest dose tested, 3000 µM, PANP2 did not fully inhibit growth, which is usually indicated by an OD₆₀₀ reading below 0.1.

On the other hand, as seen in **Figure 3c**, S-PANP2 elicited a visible and strong dose response from PA14. At over 1000 µM S-PANP2, full inhibition of PA14 was achieved. We determined that the 25% PA14 inhibition concentration of S-PANP2 was 55 µM. To explore our interest in PANP2, we also tested it at 55 µM.

Library Growth Experiment

During the library growth experiment, all replicates across conditions grew to saturation. The PA14 CRISPRi library largely grew and turned the medium a turbid white-gray color from the originally clear medium. However, after the second dilution (after T1), one of the positive control replicates turned an ocean-blue color. This is likely due to the production of siderophores and pigments, which are often signs of *P. aeruginosa* stress²⁴.

After DNA extraction and low-cycle PCR amplification of the single guide RNA (sgRNA) and Illumina adapter region was confirmed by analysis of PCR products using gel electrophoresis. **Figure 4** shows a sample gel containing PCR products from the library growth experiment. According to the Peters lab, the expected product is 276 base pairs (bp) long (unpublished). We were able to visualize the PCR products of all of our samples, and the bands appeared slightly below the 300 bp marker in the ladder, confirming that we amplified our expected product. Furthermore, our amplification was specific, as our product was the sole PCR amplification band shown on the gels. A second band that shows up below the smallest DNA ladder marker (< 100 bp) for all samples is the PCR primers. It is the only band that appears in the negative control lane (**Figure 4**).

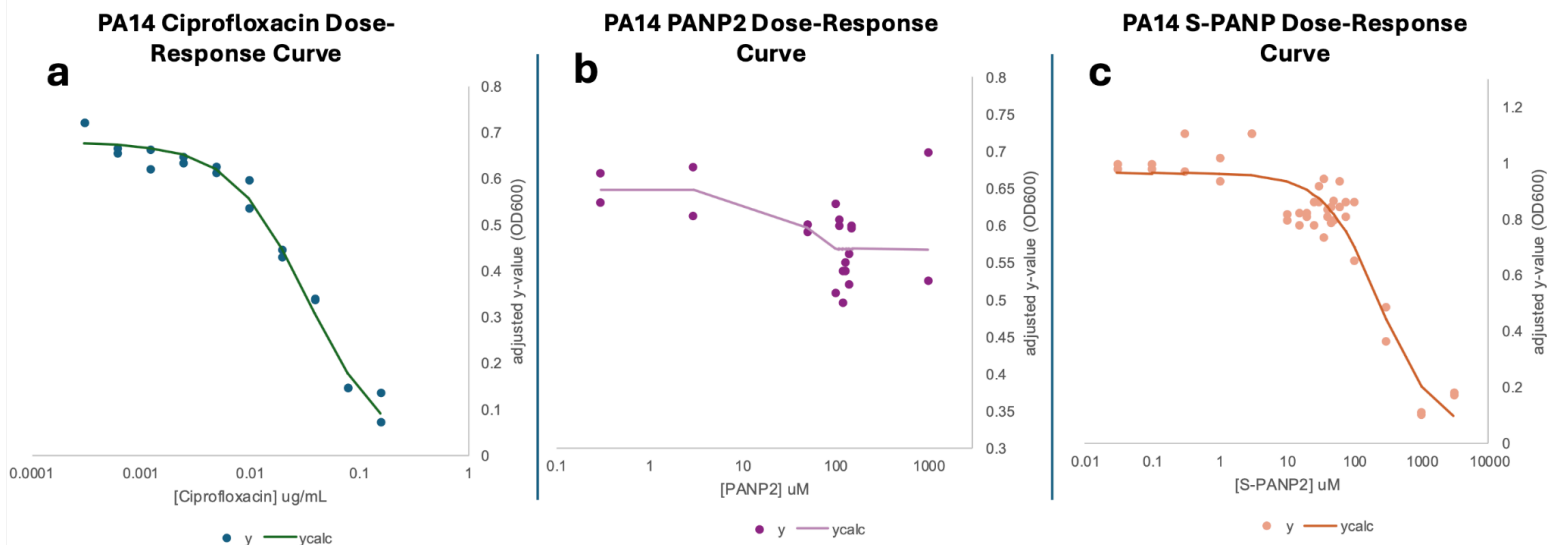


Figure 3. Dose-Response Curves for Ciprofloxacin (a), PANP2 (b), and S-PANP2. Inhibition assays were performed to test WT PA14's dose-response to a range of compound concentrations, testing additional concentrations near the suspected 25% inhibition concentration. In 96-well plates, MOPS EZRDM + 40 mM succinate media was inoculated with WT PA14 at a starting OD₆₀₀ of 0.1 alongside the experimental concentration of each compound of interest. After overnight incubation, OD₆₀₀ values were obtained, and values were fit to a sigmoid fitting curve¹⁵ to generate dose response curves. WT PA14 25% inhibition values were determined to be: (a) 0.009 ug/mL (b) N/A (c) 55 uM.

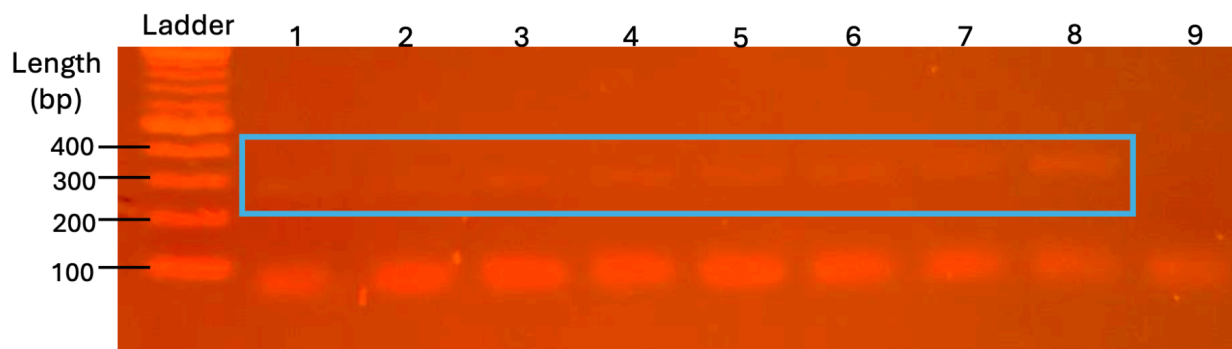


Figure 4. Image of Agarose Gel Containing Amplified sgRNAs. After the library growth experiment, the sgRNAs from PA14 CRISPRi growth conditions were amplified using low-cycle PCR with Q5 Polymerase (NEB). All PCR products were visualized using a 2% agarose gel (only a subset shown here). A NEB 1kb Plus DNA ladder was used. The blue box highlights the expected 276 bp product (lanes 1-8), which is absent in the negative control (lane 9).

Identification of PA14 Genes Sensitive and Resistant to Ciprofloxacin

In all samples, we identified gene hits that had a net \log_2FC of at least 1 and a p-value, or False Discovery Rate (FDR), below 0.05. In total, 49 gene knockdowns were found to increase PA14 susceptibility to ciprofloxacin, while 52 gene knockdowns increased PA14 survivability in response to ciprofloxacin. Negative \log_2FC s ranged from -2.582 to -1.003, while positive \log_2FC s ranged from 1.005 to 2.992. A volcano plot detailing the \log_2FC s and $\log FDR$ s of all the genes that were not filtered out by the *filterByExpr* function in edgeR for the positive control condition is shown in **Figure 5a**. The volcano plot does include genes with a net \log_2FC below 1, and the data are compared to the negative control.

Of the 49 susceptibility gene knockdown hits, we identified 48 and classified them into the following groups: DNA replication, DNA repair, translation, transmembrane transport, outer membrane structure, motility/chemotaxis, and metabolism/miscellaneous. Miscellaneous hits include metabolic genes and global regulation genes, as well as single hits that did not fall into other categories, such as a bacteriophage DNA excision gene. Furthermore, of the 8 transmembrane transport hits, 5 were related to multidrug efflux pumps. A distribution of the hits is visualized in **Figure 5b**. The largest class of genes that increased ciprofloxacin susceptibility was outer membrane structure, including genes relating to the C39 family peptidases, lipopolysaccharide assembly lipoproteins, and proteins necessary to maintain outer membrane asymmetry and integrity.

In general, gene knockdowns that increased PA14 survivability in the presence of ciprofloxacin were largely efflux pump repressor genes and ribosomal and translation-related genes. Furthermore, ciprofloxacin targets type II topoisomerases, which induce negative supercoiling in DNA²⁵. DNA gyrase is one such target, and the subunit genes *gyrA* and *gyrB* were found to have positive \log_2FC s of 1.172 and 1.027, respectively.

Some Genes Are Sensitive To All Conditions

Overall, PA14 genes that had increased fitness were condition-specific. For instance, nearly all the top 50 genes that had increased fitness in the PANP2 condition were not found to be in the top 50 genes with increased fitness in the positive control or S-PANP2 conditions. Conversely, many of the same knocked-down genes were found to have increased sensitivity across two or all conditions relative to the negative control. For instance, among the 48 identified negative \log_2FC hits in the positive control, only 17 are unique hits. Another 17 genes were also found in the top 50 negative \log_2FC hits across all three conditions. A pie chart breakdown of the general category these genes fall into is displayed in **Figure 6**. Fifty three percent of these all-condition susceptible knock-down genes were related to outer membrane structure.

Lastly, 13 knock-down genes were among the top 50 negative \log_2FC hits in only the PANP conditions. Notably, nearly half of these genes are related to DNA repair, such as all excinuclease ABC subunits and several Holliday junction branch migration proteins, which participate in nucleotide excision repair²⁶ and homologous recombination repair²⁷, respectively. A full list of the top 50 positive and negative \log_2FC gene hits across all conditions can be found in **Table S1a-f**.

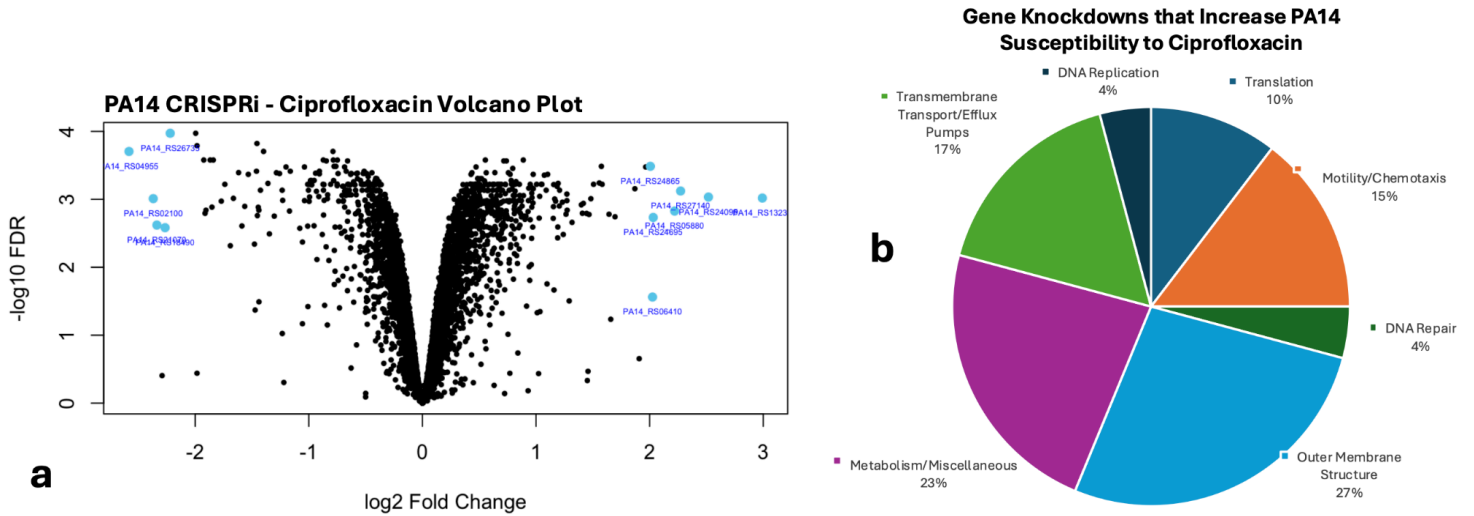


Figure 5. Ciprofloxacin (a) CRISPRi Volcano Plot and (b) Categorical Breakdown of Top 50 Gene Knockdowns that Reduced Fitness. (a) The volcano plot was created after positive control condition sgRNA barcodes were counted and processed using *edgeR*. Data was filtered and normalized relative to the negative control. The x-axis shows the \log_2 Fold Change (FC) of genes, while the y-axis shows the $-\log_{10}$ False Discovery Rate (FDR). Each point corresponds to a gene, and points with \log_2 FC > 2 and FDR < 0.05 are labeled for viewing. (b) The top 50 susceptibility gene hits with FDR < 0.05 were identified and sorted into overarching groups, such as Motility, Outer Membrane Structure, and more.

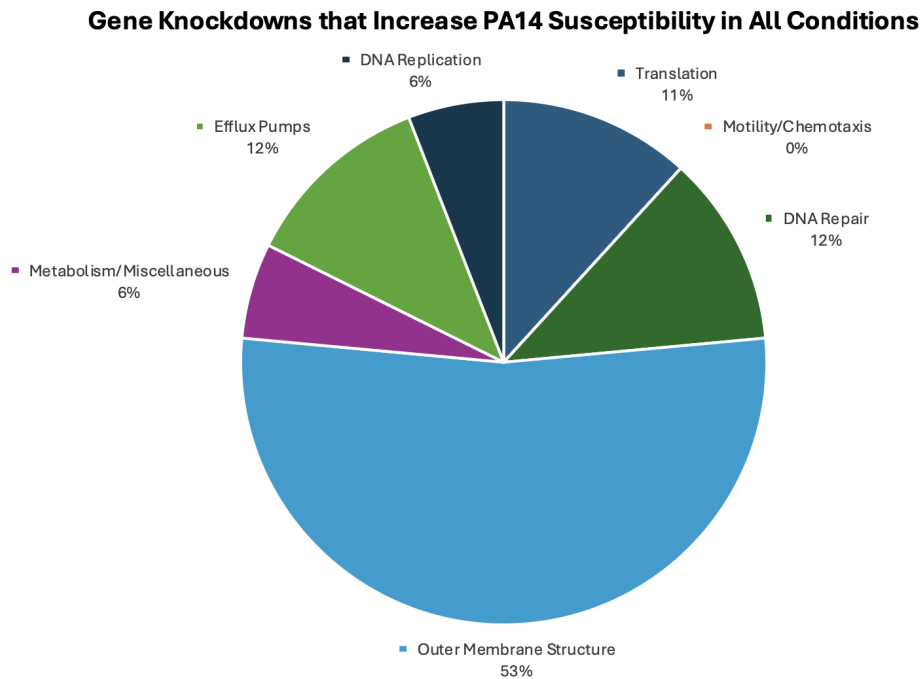


Figure 6. Breakdown of Knocked-Down Genes that Are Depleted in All Conditions. Upon analyzing the top 50 susceptibility hits across the positive control, PANP2, and S-PANP2 conditions, 17 genes were found to be depleted in all three conditions. Over half of the identified genes are related to PA14 cellular outer membrane structure.

Identification of PA14 Genes Sensitive and Resistant to PANP2

In total, 118 gene knockdowns were found to increase PA14 susceptibility to PANP2, while 48 gene knockdowns increased PA14 survivability. Negative \log_2 FCs ranged from -9.098 to -1.002, while positive \log_2 FC values ranged from 1.022 to 2.044. A volcano plot showing the differential distribution of all filtered genes (which also includes genes with a net \log_2 FC change below 1) relative to the negative control condition is shown in **Figure 7a**.

Of the top 50 susceptibility gene knockdown hits, we classified them into the same groups shown in **Figure 5**. Metabolism/miscellaneous hits again represent non-specific hits or single hits that don't fit well into other categories. It includes transcriptional regulators for specific genes, such as *alpR*, a transcriptional regulator for PA14's cell death pathway. This group also contains enzymes and proteins in more general pathways, such as ornithine carbamoyltransferase, which is involved in anabolic and catabolic arginine metabolism²⁸, as well as a protein identified as a non-specific cold shock protein. Our largest specific group was genes and proteins related to the membrane structure and integrity of PA14 cells (**Figure 7b**). Lastly, of the transmembrane transport hits, 2 of the 5 total hits were related to multidrug efflux pumps.

In general, gene knockdowns that increased PA14 survivability in the presence of PANP2 were largely flagella-related genes, such as those encoding the flagellar motor switch proteins FliN and FliM, as well as flagellin. Genes relating to flagellar expression and proteins comprised over 50% of the 48 gene knockdown hits that increased PA14 survivability in the presence of PANP2. Other hits mainly include efflux pump repressor genes.

Identification of PA14 Genes Sensitive and Resistant to S-PANP2

In total, we found 144 gene knockdowns that increase PA14 susceptibility to S-PANP2, while 210 gene knockdowns increased PA14 survivability by a \log_2 FC of at least 1. Negative \log_2 FCs ranged from -7.047 to -1.009, while positive \log_2 FCs ranged from 1.003 to 7.873. Again, a volcano plot showing the differential distribution of all non-filtered genes relative to the negative control condition is shown in **Figure 8a**.

Of the top 50 susceptibility gene knockdown hits, we identified 49, as one encoded for a protein containing a domain of unknown function. We again classified the hits into the same groups previously used. Our largest group is related to transmembrane transport (**Figure 8b**). Hits included *to/Q*, which encodes a translocation protein responsible for transporting large molecules across the cell membrane²⁹. Other hits included lipopolysaccharide transporters and outer membrane enzymes for protein modification. Lastly, of these hits, 5 of the 11 total hits were related to drug resistance efflux pumps.

Overall, the top 50 gene knockdowns that increased PA14 survival in the presence of S-PANP were varied, but there was a trend of knockdowns relating to translation, such as knockdowns of ribosomal proteins or tRNAs. For instance, the genes for the 50S ribosomal subunit protein L36 and the 30S ribosomal subunit protein S7 had \log_2 FCs of 7.741 and 7.446, respectively.

Discussion

Growing antimicrobial resistance is driving a need for the development of novel antimicrobial agents to treat pathogens such as *Pseudomonas aeruginosa*^{1,4,5,6}. Here, we utilized a CRISPRi library growth and data analysis protocol to work towards identifying *P. aeruginosa* PA14's sensitive targets to a novel natural product, which we call PANP2, and a semi-synthetic derivative, S-PANP2.

Experiment and Positive Control Validity

According to the Ward et al. paper we followed to conduct this CRISPRi library growth experiment¹¹, their positive controls were validated by confirming that the known gene targets of their positive control antibiotics were significantly depleted following the growth protocol. Following this logic, we predicted that genes relating to DNA gyrase, the target of ciprofloxacin, would be significantly depleted. However, we instead found that the subunit genes *gyrA* and *gyrB* had positive log₂FCs.

Although these results contradict what we initially expected, we still find evidence that our positive control conditions worked and show the validity of our PA14 CRISPRi experiment. One possible explanation is that *gyrA* and *gyrB* knockdowns conferred increased fitness to PA14 in the presence of subinhibitory concentrations of ciprofloxacin. This may be due to the DNA gyrase knockdown strains having less gyrase to be targeted by ciprofloxacin, making other strains with full levels of gyrase expression easier targets for the antibiotic. In a recent study, researchers found that partial CRISPRi knockdowns could enhance fitness in stressful conditions, although they performed their tests using cyanobacteria³⁰.

However, a finding that supports Ward et al.'s findings is the depletion of a ParA family protein involved in plasmid partitioning. It is a unique susceptibility hit to the positive control condition, with a log₂FC of -1.478. ParA is reported to be an allele of *gyrB*³¹, one of our expected depletion targets. Thus, it is possible that ParA was more susceptible to ciprofloxacin in our PA14 CRISPRi library. Furthermore, we are reassured by the finding that knocking down an *nfxB* efflux pump repressor gene increases fitness in the presence of ciprofloxacin (log₂FC = 2.006). The NfxB protein helps confer resistance to quinolone antibiotics like ciprofloxacin³², so it makes sense that knocking its repressor down increases fitness because NfxB can be expressed more, making the cell more resistant to quinolone antibiotics.

Traditionally, CRISPRi-based chemical genomic screens are focused on identifying sensitizing knockdowns to infer the compound's cellular target or stress pathways. However, as seen here and in our PANP analysis, our results highlight the complementary value of examining knockdowns that confer increased fitness. In multiple conditions, we found that knockdowns of specific functional categories, such as flagellar assembly genes, consistently promoted survival under compound treatment. These findings suggest that enrichment phenotypes can also reveal pathways that interact with or buffer the cellular response to the compound, even if they are not the direct molecular target.

Thus, analysis of increased-fitness knockdowns provides important mechanistic insights: identifying biological processes that, when disabled, mitigate compound stress. Our study supports the idea that both sensitizing and protective knockdowns contribute valuable, nonredundant information toward understanding a compound's mode of action.

PANPs Are Potent

In our results, we show that, among the top 50 hits, PA14 cells containing outer membrane structure-related knockdowns are especially susceptible to PANP2, while transmembrane transport-related knockdowns were more susceptible to S-PANP2. However, it is again worth noting that many of the same genes were susceptibility hits across all conditions. This may be indicative of general genetic vulnerabilities and antibiotic sensitivities present in *P. aeruginosa*. In other words, knocking down these genes may make *P. aeruginosa* more susceptible to general antibiotic-induced stress conditions. For instance, outer membrane structure genes, such as *lptE* and *ompH*, made up the largest group of genes sensitive to all conditions. It can be reasoned that, by knocking down genes that contribute to membrane structure, rigidity, and permeability, those PA14 CRISPRi knockdown strains become more susceptible to ciprofloxacin and our PANPs because those compounds can more easily enter the cell.

Assuming that these shared susceptibility hits are revealing genetic vulnerabilities within PA14, we find that our PANPs' potencies are extremely promising. This is supported by the fact that all susceptibility hits have a greater magnitude of \log_2FC in PANP conditions relative to the positive control condition. For example, the top susceptibility gene for the positive control and PANP2 condition was PA14_RS04955, which encodes a tRNA-Leucine ligase enzyme. Its \log_2FC in the ciprofloxacin condition was -2.583, whereas the corresponding values in the PANP2 and S-PANP2 conditions are -9.098 and -5.371, respectively. This shows that our PANPs are able to induce a greater magnitude of depletion across susceptible knockdowns. This is impressive because these changes were induced at a 25% inhibitory concentration for all conditions except for PANP2, which was tested at a concentration assumed to be much lower than its true PA14 25% inhibition concentration. This suggests that our PANPs are extremely potent, and PA14 may be more susceptible to them in comparison to ciprofloxacin, a prescription antibiotic.

PANPs May Target DNA Repair

PANP2 and S-PANP2 also have several susceptibility hits exclusively shared between them. Notably, 13 of the top 50 susceptible gene targets were unique to PANP conditions. The chemical core, identical between our PANPs, may be responsible for these shared observations.

Interestingly, both compounds produced susceptibility hits across all three subunits of the excinuclease ABC complex (*uvrA*, *uvrB*, and *uvrC*). Excinuclease ABC is a critical component of the bacterial nucleotide excision repair pathway, which is responsible for detecting and repairing bulky DNA lesions²⁶. The consistent depletion of excinuclease ABC subunit knockdowns under treatment suggests that cells deficient in DNA repair machinery become selectively vulnerable to PANPs.

This pattern reflects synthetic lethality, where inhibition of two separate pathways, chemical stress from the compound and genetic knockdown of excision repair, results in "lethality" (rather, decreased fitness), whereas disruption of either alone is survivable. The fact that this vulnerability is observed across all of the protein subunits in both compounds strongly suggests that the core scaffold may interfere with DNA integrity, either by causing DNA damage

directly or by obstructing repair processes. This is further supported by the shared susceptibility hits of Holliday junction branch protein genes²⁷.

Overall, the sensitivity of DNA repair-knockdown strains points toward a mechanistic link between the chemical core structure and DNA repair pathways^{26,27}, providing an important clue for understanding the compounds' mode of action.

PANP2 May Specifically Target *P. aeruginosa* Biofilm Scaffolding

Among the top 50 gene knockdowns found to increase PA14 susceptibility to PANP2, the identified genes did not point to any clear specific target. Hits unique to only the PANP2 conditions were varied, including genes involved in DNA replication (example: DNA polymerase IV), DNA repair (helicase *recG*), and translation (ribosome silencing factor *rsfS*) (**Table S1c**). However, upon looking at the gene knockdowns that conferred greater fitness against PANP2, nearly half of the top 50 hits are related to flagella, and all hits are unique to the PANP2 condition (**Table S1d**).

Flagella of *P. aeruginosa* contribute to motility and biofilm formation. They also play major roles in adhesion to surfaces, especially for adhesion to mucus in the lungs of cystic fibrosis patients³³. In a 2021 study, Ozer et al. tracked *P. aeruginosa* flagella in biofilm life cycles via genetic code expansion and flagella knockout studies. They found that flagella are continuously synthesized within growing biofilms and provided evidence that flagella contribute to the strength of the biofilm's structure³⁴. Thus, if PA14 cells with flagella-related gene knockdowns have increased fitness against PANP2, then PANP2 may function by targeting *P. aeruginosa* flagella within biofilms. This proposed mechanism also aligns with our observations that PANPs are potent biofilm inhibitors (**Figure 1**), but PANP2 is a poor bacteriostatic or bactericidal compound (**Figure 3a**). Thus, PANP2 may not be toxic to basic metabolism or survival, but it is a strong biofilm inhibitor because it disrupts the biofilm/sessile cell state. Overall, we propose that, because PANP2 interferes with biofilm formation without strongly affecting cell survival, we primarily see protective effects from gene knockdowns and relatively little directed sensitization across the genome.

S-PANP2 May Inhibit *P. aeruginosa* During Active Growth

Similar to the PANP2 condition, gene knockdowns that conferred increased survivability in the presence of a compound of interest told more of a story than the susceptibility hits. Of the top 50 gene knockdowns that increased fitness in the presence of S-PANP2, 7 were directly related to the ribosome, with another 7 being related to translation through encoding proteins related to amino acid synthesis (aspartokinase), tRNAs, translation termination regulation (peptide chain release factor 1), etc. Most of these hits were also solely associated with the S-PANP2 condition (**Table S1f**).

Thus, it is possible that S-PANP2 more directly targets the ribosome and protein synthesis/translation. This makes sense, given that S-PANP2 contains an amino acid-like moiety. This modification may be somehow interrupting translation by mimicking amino acids, stalling the ribosome, or prematurely terminating protein synthesis. Thus, by having translation-related knockdowns that slow protein synthesis by slowing the ribosome or having

fewer tRNAs available, these CRISPRi knockdown hits may have increased fitness because they can evade the translation interference mechanism of S-PANP2.

This proposed mechanism of action may also explain why S-PANP2 is more effective at killing or inhibiting PA14 growth (**Figure 3c**). It targets actively growing cells, which is reflected by active protein synthesis. Because protein synthesis is more necessary for cell survival, this may explain why S-PANP2 is a better bacteriostatic/bactericidal compound than PANP2.

Limitations and Future Directions

While our CRISPRi chemical genetic screens identified a number of promising sensitizing and protective hits against our PANPs, further in-depth analysis is necessary to fully interpret the biological pathways involved. In particular, several genes and pathways of interest, including transcriptional regulators, siderophore biosynthesis genes, and pigment-related genes, were initially grouped into broad functional categories such as "Metabolism/Miscellaneous" and warrant further investigation to clarify their potential roles in compound susceptibility. In fact, we initially predicted that our compounds would hinder *P. aeruginosa* pigment and siderophore production, and we are interested in further exploring how our PANPs potentially interfere with these pathways.

A significant limitation was the time constraint associated with manually mapping gene identifiers/codes to specific gene or protein names, which limited the throughput of our pathway analyses. Future work could potentially incorporate automated annotation pipelines or targeted validation of key hits to accelerate this process.

Additionally, our current analysis treated all sgRNAs equally, without accounting for mismatch guides. Although this simplified analysis provided an overall view of fitness effects, examining guide fidelity and mismatches more carefully could refine hit confidence and uncover potential off-target effects. In future data analyses, incorporating mismatch-aware guide assignment and refining barcode association may improve the specificity and resolution of the screen.

Finally, to further validate our experimental approach, another next step would be to explore additional well-characterized antibiotics as positive controls against the PA14 CRISPRi library. Screening with compounds that have distinct and well-understood mechanisms of action could help confirm the system's ability to correctly identify expected targets and refine baseline expectations for interpreting new compound-specific effects.

Works Cited

1. Ventola, C. L. (2015). The antibiotic resistance crisis. *Pharmacy and Therapeutics*, 40(4), 277–283. <https://www.ncbi.nlm.nih.gov/pmc/articles/PMC4378521/>
2. Brüssow, H. (2024). The antibiotic resistance crisis and the development of new antibiotics. *Microbial Biotechnology*, 17(7), e14510. <https://doi.org/10.1111/1751-7915.14510>
3. Murray, C. J. L., Ikuta, K. S., Sharara, F., Swetschinski, L., Robles Aguilar, G., Gray, A., Han, C., Bisignano, C., Rao, P., Wool, E., Johnson, S. C., Browne, A. J., Chipeta, M. G., Fell, F., Hackett, S., Haines-Woodhouse, G., Kashef Hamadani, B. H., Kumaran, E. A. P., McManigal, B., ... Naghavi, M. (2022). Global burden of bacterial antimicrobial resistance in 2019: A systematic analysis. *The Lancet*, 399(10325), 629–655. [https://doi.org/10.1016/S0140-6736\(21\)02724-0](https://doi.org/10.1016/S0140-6736(21)02724-0)
4. World Health Organization. Prioritization of Pathogens to Guide Discovery, Research and Development of New Antibiotics for Drug-Resistant Bacterial Infections, Including Tuberculosis. World Health Organization; Geneva, Switzerland: 2017.
5. Tuon, F. F., Dantas, L. R., Suss, P. H., & Tasca Ribeiro, V. S. (2022). Pathogenesis of the *Pseudomonas aeruginosa* biofilm: A review. *Pathogens*, 11(3), 300. <https://doi.org/10.3390/pathogens11030300>
6. Thi, M. T. T., Wibowo, D., & Rehm, B. H. A. (2020). *Pseudomonas aeruginosa* Biofilms. *International Journal of Molecular Sciences*, 21(22), 8671. <https://doi.org/10.3390/ijms21228671>
7. Pradeep, S., & Arratia, P. E. (2022). To biofilm or not to biofilm. *eLife*, 11, e80891. <https://doi.org/10.7554/eLife.80891>
8. Moloney, M. G. (2016). Natural products as a source for novel antibiotics. *Trends in Pharmacological Sciences*, 37(8), 689–701. <https://doi.org/10.1016/j.tips.2016.05.001>
9. Grace, A., Sahu, R., Owen, D. R., & Dennis, V. A. (2022). *Pseudomonas aeruginosa* reference strains PAO1 and PA14: A genomic, phenotypic, and therapeutic review. *Frontiers in Microbiology*, 13. <https://doi.org/10.3389/fmicb.2022.1023523>
10. Peters, J. M., Koo, B.-M., Patino, R., Heussler, G. E., Hearne, C. C., Qu, J., Inclan, Y. F., Hawkins, J. S., Lu, C. H. S., Silvis, M. R., Harden, M. M., Osadnik, H., Peters, J. E., Engel, J. N., Dutton, R. J., Grossman, A. D., Gross, C. A., & Rosenberg, O. S. (2019). Enabling genetic analysis of diverse bacteria with Mobile-CRISPRi. *Nature Microbiology*, 4(2), 244–250. <https://doi.org/10.1038/s41564-018-0327-z>
11. Ward, R. D., Tran, J. S., Banta, A. B., Bacon, E. E., Rose, W. E., & Peters, J. M. (2024). Essential gene knockdowns reveal genetic vulnerabilities and antibiotic sensitivities in *Acinetobacter baumannii*. *mBio*, 15(2), e02051-23. <https://doi.org/10.1128/mbio.02051-23>
12. *Ez rich defined medium*. (n.d.). Retrieved April 29, 2025, from <https://www.genome.wisc.edu/resources/protocols/ezmedium.htm>
13. Ezraty, B., Henry, C., Hérisse, M., Denamur, E., & Barras, F. (2014). Commercial Lysogeny Broth culture media and oxidative stress: A cautious tale. *Free Radical Biology and Medicine*, 74, 245–251. <https://doi.org/10.1016/j.freeradbiomed.2014.07.010>
14. *Ciprofloxacin, 98%, thermo scientific chemicals*. (n.d.). Retrieved April 30, 2025, from <https://www.thermofisher.com/order/catalog/product/J61317.06>
15. Kemmer, G., & Keller, S. (2010). Nonlinear least-squares data fitting in Excel spreadsheets. *Nature Protocols*, 5(2), 267–281. <https://doi.org/10.1038/nprot.2009.182>
16. Qu, J., Prasad, N. K., Yu, M. A., Chen, S., Lyden, A., Herrera, N., Silvis, M. R., Crawford, E., Looney, M. R., Peters, J. M., & Rosenberg, O. S. (2019). Modulating pathogenesis with mobile-crispri. *Journal of Bacteriology*, 201(22). <https://doi.org/10.1128/JB.00304-19>
17. 262588213843476. (n.d.). *Strategy to count barcodes*. Gist. Retrieved April 29, 2025, from <https://gist.github.com/ryandward/ed9bb3d3414f4eed17ad58fe6da1ed7a>

18. Karp, P. D., Billington, R., Caspi, R., Fulcher, C. A., Latendresse, M., Kothari, A., Keseler, I. M., Krummenacker, M., Midford, P. E., Ong, Q., Ong, W. K., Paley, S. M., & Subhraveti, P. (2019). The BioCyc collection of microbial genomes and metabolic pathways. *Briefings in Bioinformatics*, *20*(4), 1085–1093. <https://doi.org/10.1093/bib/bbx085>
19. Altschul, S. F., Gish, W., Miller, W., Myers, E. W., & Lipman, D. J. (1990). Basic local alignment search tool. *Journal of Molecular Biology*, *215*(3), 403–410. [https://doi.org/10.1016/S0022-2836\(05\)80360-2](https://doi.org/10.1016/S0022-2836(05)80360-2)
20. Riquelme, S. A., & Prince, A. (2020). Airway immunometabolites fuel *Pseudomonas aeruginosa* infection. *Respiratory Research*, *21*, 326. <https://doi.org/10.1186/s12931-020-01591-x>
21. Rojo, F. (2010). Carbon catabolite repression in *Pseudomonas*: Optimizing metabolic versatility and interactions with the environment. *FEMS Microbiology Reviews*, *34*(5), 658–684. <https://doi.org/10.1111/j.1574-6976.2010.00218.x>
22. Sonnleitner, E., Abdou, L., & Haas, D. (2009). Small RNA as global regulator of carbon catabolite repression in *Pseudomonas aeruginosa*. *Proceedings of the National Academy of Sciences*, *106*(51), 21866–21871. <https://doi.org/10.1073/pnas.0910308106>
23. Mould, D. L., Stevanovic, M., Ashare, A., Schultz, D., & Hogan, D. A. (2022). Metabolic basis for the evolution of a common pathogenic *Pseudomonas aeruginosa* variant. *eLife*, *11*, e76555. <https://doi.org/10.7554/eLife.76555>
24. Lan, L., Murray, T. S., Kazmierczak, B. I., & He, C. (2010). *Pseudomonas aeruginosa* OspR is an oxidative stress sensing regulator that affects pigment production, antibiotic resistance and dissemination during infection. *Molecular Microbiology*, *75*(1), 76–91. <https://doi.org/10.1111/j.1365-2958.2009.06955.x>
25. Thai, T., Salisbury, B. H., & Zito, P. M. (2025). Ciprofloxacin. In *StatPearls*. StatPearls Publishing. <http://www.ncbi.nlm.nih.gov/books/NBK535454/>
26. Selby, C. P., & Sancar, A. (1990). Structure and function of the (A)BC excinuclease of *Escherichia coli*. *Mutation Research*, *236*(2–3), 203–211. [https://doi.org/10.1016/0921-8777\(90\)90005-p](https://doi.org/10.1016/0921-8777(90)90005-p)
27. Rish, A. D., Shen, Z., Chen, Z., Zhang, N., Zheng, Q., & Fu, T.-M. (2023). Molecular mechanisms of Holliday junction branch migration catalyzed by an asymmetric RuvB hexamer. *Nature Communications*, *14*(1), 3549. <https://doi.org/10.1038/s41467-023-39250-6>
28. Itoh, Y., Soldati, L., Stalon, V., Falmagne, P., Terawaki, Y., Leisinger, T., & Haas, D. (1988). Anabolic ornithine carbamoyltransferase of *Pseudomonas aeruginosa*: Nucleotide sequence and transcriptional control of the *argF* structural gene. *Journal of Bacteriology*, *170*(6), 2725–2734. <https://doi.org/10.1128/jb.170.6.2725-2734.1988>
29. Lafontaine, E. R., & Sokol, P. A. (1998). Effects of iron and temperature on expression of the *Pseudomonas aeruginosa* *tolQRA* genes: Role of the ferric uptake regulator. *Journal of Bacteriology*, *180*(11), 2836–2841. <https://doi.org/10.1128/JB.180.11.2836-2841.1998>
30. Hren, A., Lollini, N., Carper, D. L., Abraham, P. E., Cameron, J. C., Fox, J. M., & Eckert, C. A. (2025). High-density CRISPRi screens reveal diverse routes to improved acclimation in cyanobacteria. *Proceedings of the National Academy of Sciences*, *122*(12), e2412625122. <https://doi.org/10.1073/pnas.2412625122>
31. Menzel, R., & Gellert, M. (1994). The biochemistry and biology of dna gyrase. In L. F. Liu (Ed.), *Advances in Pharmacology* (Vol. 29, pp. 39–69). Academic Press. [https://doi.org/10.1016/S1054-3589\(08\)60539-6](https://doi.org/10.1016/S1054-3589(08)60539-6)
32. Shiba, T., Ishiguro, K., Takemoto, N., Koibuchi, H., & Sugimoto, K. (1995). Purification and characterization of the *Pseudomonas aeruginosa* NfxB protein, the negative regulator of the *nfxB* gene. *Journal of Bacteriology*, *177*(20), 5872–5877. <https://doi.org/10.1128/jb.177.20.5872-5877.1995>

33. Valentin, J. D. P., Straub, H., Pietsch, F., Lemare, M., Ahrens, C. H., Schreiber, F., Webb, J. S., van der Mei, H. C., & Ren, Q. (2022). Role of the flagellar hook in the structural development and antibiotic tolerance of *Pseudomonas aeruginosa* biofilms. *The ISME Journal*, 16(4), 1176–1186. <https://doi.org/10.1038/s41396-021-01157-9>
34. Ozer, E., Yaniv, K., Chetrit, E., Boyarski, A., Meijler, M. M., Berkovich, R., Kushmaro, A., & Alfonta, L. (2021). An inside look at a biofilm: *Pseudomonas aeruginosa* flagella biotracking. *Science Advances*, 7(24), eabg8581. <https://doi.org/10.1126/sciadv.abg8581>

SI

Available Upon Request. Please contact tim.bugni@wisc.edu or shrrw8@gmail.com.